JOURNAL OF COMPUTATIONAL PHYSICS **38**, 185–211 (1980)

Implementing Hamilton's Law of Varying Action with Shifted Legendre Polynomials

DONALD L. HITZL

Lockheed Palo Alto Research Laboratory, Dept. 52–56, Bldg. 580, 3460 Hillview Ave., Palo Alto, California 94304

Received August 20, 1979; revised December 3, 1979

The "Law of Varying Action," originally published by Hamilton in 1834, was recently employed by Bailey to generate power series solutions characterizing the motions of dynamical systems. Furthermore, this method enables the approximating series to be constructed in a simple and direct way, without using the associated differential equations of motion. The implementation of this new technique is presented here using, instead of ordinary power series, series with Shifted Legendre Polynomials as basis functions. The theory and applications are described in detail and numerical results are presented for two problems—(i) a lightly damped harmonic oscillator with one degree of freedom, (ii) two periodic orbits of the restricted three-body problem. The far superior performance of the Shifted Legendre Polynomial series is confirmed in both examples.

INTRODUCTION

Recently, Bailey [1, 2] made a rather surprising discovery regarding what is commonly referred to as "Hamilton's Principle." Upon examining Hamilton's original papers [3, 4] of 1834 and 1835 concerning "a general method in dynamics," Bailey reached the conclusion that Hamilton had not formulated this principle but had instead developed a more comprehensive theory which he called "The Law of Varying Action" [3, pp. 249–253]. This Law of Varying Action yields approximate solutions of initial value problems associated with dynamical systems, and does so without any reference to differential equations of motion.

In a previous paper [5] it was demonstrated how the law of varying action can be used to obtain approximate solutions of the well-known restricted three-body problem by using ordinary power series in the independent (time) variable. The purpose of this paper is to present the implementation of this new technique using Shifted Legendre Polynomials P_n^* ($n = 0, 1, 2, \ldots$) as basis functions [6–8] for the approximating series. Indeed, it has been found that earlier difficulties with accuracy and convergence using ordinary power series have been totally eliminated by employing series in terms of these orthogonal polynomials. In particular, the necessary inverse of a rather large matrix is now determined with high precision in all cases whereas, previously, this matrix was rather poorly conditioned.

0021-9991/80/140185–27$02.00/0

581/38/2-5

This paper is structured as follows. First, Hamilton's Law of Varying Action is developed in its most general form. Second, series solutions are formulated for both a simple damped harmonic oscillator and for planar orbit motion in the restricted three-body problem. Third, numerical results are included for both example problems confirming the far superior performance of the Shifted Legendre Polynomial series in these applications.

Hamilton's Law of Varying Action

By proceeding as follows[1], a version of Hamilton's Law of Varying Action can be obtained that is not encumbered by any appeal to the calculus of variations[2] and, furthermore, is somewhat more general than that provided by Bailey.

Let K denote the kinetic energy of a holonomic dynamical system characterized by generalized coordinates $q_1,..., q_n$, let $s_1,..., s_n$ be any functions of the time t, and introduce the function Φ as

$$\Phi \triangleq \sum_{k=1}^{n} \left[\left(\frac{\partial K}{\partial q_k} + F_k\right) s_k + \frac{\partial K}{\partial \dot{q}_k} \dot{s}_k\right], \tag{1}$$

where F_k is the generalized active force associated with q_k $(k = 1,..., n)$. Integration of both sides of Eq. (1) with respect to time from $t = t_1$ to $t = t_2$ then gives

$$\int_{t_1}^{t_2} \Phi \, dt = \int_{t_1}^{t_2} \sum_{k=1}^{n} \left[\left(\frac{\partial K}{\partial q_k} + F_k\right) s_k + \frac{\partial K}{\partial \dot{q}_k} \dot{s}_k\right] dt. \tag{2}$$

Interchanging the order of integration and summation on the right-hand side and subsequently integrating the term $(\partial K/\partial \dot{q}_k)\, \dot{s}_k$ by parts yields

$$\int_{t_1}^{t_2} \Phi \, dt = \sum_{k=1}^{n} \left\{\int_{t_1}^{t_2} \left[-\frac{d}{dt}\left(\frac{\partial K}{\partial \dot{q}_k}\right) + \frac{\partial K}{\partial q_k} + F_k\right] s_k \, dt + \frac{\partial K}{\partial \dot{q}_k} s_k \Big|_{t_1}^{t_2}\right\} \tag{3}$$

The term in square brackets in Eq. (3) vanishes by virtue of Lagrange's equations, leaving the relation

$$\int_{t_1}^{t_2} \Phi \, dt - \sum_{k=1}^{n} \frac{\partial K}{\partial \dot{q}_k} s_k \Big|_{t_1}^{t_2} = 0, \tag{4}$$

which is a statement of Hamilton's Law of Varying Action in its most general form.

Several additional comments are now in order. First we note that Eq. (4) is

[1] This idea is due to Professor T. R. Kane of Stanford University.

[2] A fundamental tenet in Bailey's work [9] is that the concepts for the calculus of variations resulted in the simplification of Hamilton's Law to Hamilton's Principle and this, in turn, caused others to miss the computational possibilities inherent in Hamilton's Law.

applicable to nonconservative as well as conservative dynamical systems. Further, nonstationary problems having time-variable parameter values or other non-constant properties can also be handled easily using Eq. (4) [1, pp. 443–449]. Second, it is important to observe that Hamilton's Law is a fundamental principle governing the motion of dynamical systems. Quoting from [1, p. 437], the significance of Eq. (4) is: "The natural path and/or configuration of a system of particles or a continuum will be that for which the time integral of the work of all forces acting, both natural and applied, is a minimum." Third, we see that Eq. (4) does not require any knowledge of the underlying differential equations of motion. The power of Hamilton's Law is simply that *exact* solutions of Eq. (4) necessarily satisfy the equations of motion. Furthermore, Bailey has performed checks [1, pp. 443–447; 2, p. 1156] verifying that approximate analytical solutions obtained from Eq. (4) do indeed satisfy the differential equations of motion to a fairly high precision (maximum error of a few hundredths of 1 %). Accuracy checks are also included for the two example problems treated in this paper.

For further descriptive material, the reader is referred to [1, 2, 9] together with the references included therein. In the next section, the use of Eq. (4) to produce approximate solutions of dynamical problems will be described.

Approximate Solution

For a problem with three degrees of freedom with generalized coordinates q_1, q_2 and q_3, it is typically assumed that each q_i can be represented by a power series of the form

$$\mathbf{q}(t) \triangleq \begin{bmatrix} q_1(t) \\ q_2(t) \\ q_3(t) \end{bmatrix} = \mathbf{q}_0 + \dot{\mathbf{q}}_0 t + \sum_{\alpha=2}^{\alpha_f} \begin{bmatrix} A_\alpha \\ B_\alpha \\ C_\alpha \end{bmatrix} (t/t_0)^\alpha, \tag{5}$$

where

$\mathbf{q}_0 = \mathbf{q}_0(0)$ is the initial position,

$\mathbf{q}_0 = \dot{\mathbf{q}}_0(0)$ is the initial velocity,

α is the appropriate index (i, k or m) corresponding to each of the coordinates (q_1, q_2 or q_3), and

α_f is the appropriate upper limit (N, M or P).

Thus, we have in general

$$\begin{aligned} 2 \leqslant i \leqslant N \qquad &\text{for} \quad q_1(t), \\ 2 \leqslant k \leqslant M \qquad &\text{for} \quad q_2(t), \end{aligned} \tag{6}$$

and

$$2 \leqslant m \leqslant P \qquad \text{for} \quad q_3(t).$$

Also, the desired time interval for the series representation is $0 \leqslant t \leqslant t_0$ so t_0 is the final time.

Similarly, the arbitrary functions $s_k(t)$ in Eq. (4) are assumed to have the form

$$\mathbf{s}(t) \triangleq \begin{bmatrix} s_1(t) \\ s_2(t) \\ s_3(t) \end{bmatrix} = \sum_{\beta=2}^{\beta_f} \begin{bmatrix} a_\beta \\ b_\beta \\ c_\beta \end{bmatrix} (t/t_0)^\beta, \tag{7}$$

where

β is the appropriate index (j, l or n) corresponding to each of the variables (s_1, s_2 or s_3) and

β_f is the appropriate upper limit (N, M, or P) so we have again

$$\begin{aligned} 2 \leqslant j \leqslant N \quad &\text{for} \quad s_1(t), \\ 2 \leqslant l \leqslant M \quad &\text{for} \quad s_2(t), \end{aligned} \tag{8}$$

and

$$2 \leqslant n \leqslant P \quad \text{for} \quad s_3(t).$$

Then, inserting Eqs. (5) and (7) into Eq. (4) and integrating yields a matrix equation of the general form

$$\begin{bmatrix} M_{11} & M_{12} & M_{13} \\ M_{21} & M_{22} & M_{23} \\ M_{31} & M_{32} & M_{33} \end{bmatrix} \begin{bmatrix} A \\ B \\ C \end{bmatrix} = \begin{bmatrix} U(\mathbf{q}(t)) \\ V(\mathbf{q}(t)) \\ W(\mathbf{q}(t)) \end{bmatrix}, \tag{9}$$

where, because of linearity in s_k, the unknown constants a_j, b_l and c_n have cancelled out on each side of the resulting three equations in (9). The matrix M, which is of dimension $(N+M+P-3) \times (N+M+P-3)$, can be inverted once and for all while the forcing functions U_j, V_l and W_n are generally functions of the initial conditions and the unknown solution $\mathbf{q}(t)$; i.e., functions of the unknown constants A_i, B_k and C_m. This is handled quite simply on the computer, however, by iteration in the following way.

First, A_i, B_k and C_m are all set equal to zero in the functions U_j, V_l and W_n. These functions are then evaluated and Eq. (9) is solved for A_i, B_k and C_m. Finally, this procedure is repeated until the differences between successive determinations of these unknown coefficients have all become less than some prescribed value, for example, 10^{-10}.

For the two periodic orbits considered in Example II (the restricted three-body problem), convergence to this precision is usually achieved in 5 to 15 iterations. Furthermore, these iterations are simplified since M must only be inverted once. The reader is referred to [1], [2] or [5] for further details on the implementation of Eq. (4) with power series.

Now, after these preliminaries, the primary purpose of this section can be fulfilled. This is to present the assumed solution form when Shifted Legendre Polynomials P_i^* are used as basis functions. Necessary details relative to the mathematical properties of these orthogonal functions are discussed in the Appendix. Setting

$$\varkappa \triangleq t/t_0 \tag{10}$$

so $0 \leqslant \varkappa \leqslant 1$, the solution for a problem with a single degree of freedom $q(t)$ is assumed of the form

$$\begin{aligned} q(t) &= \sum_{i=0}^{N} A_i P_i^*(\varkappa) \\ &= A_0 + A_1 P_1^* + \sum_{i=2}^{N} A_i P_i^* \end{aligned} \tag{11}$$

since $P_0^*(\varkappa) \equiv 1$.

The idea is first to solve for the A_i ($i = 2, 3, \ldots, N$) and then use the known initial conditions

$$\begin{aligned} q_0 &\triangleq q(0), \\ \dot{q}_0 &\triangleq \dot{q}(0) \end{aligned} \tag{12}$$

to determine the final unknowns A_0 and A_1. In particular, consider

$$\dot{q}(0) = \left(A_1 \frac{dP_1^*}{d\varkappa} + \sum_{i=2}^{N} A_i \frac{dP_i^*}{d\varkappa} \right) \frac{d\varkappa}{dt} \bigg|_{\varkappa = t = 0}, \tag{13}$$

which is rewritten

$$\dot{q}_0 = \frac{1}{t_0} \left(2A_1 + \sum_{i=2}^{N} A_i \frac{dP_i^*}{d\varkappa} \bigg|_{\varkappa=0} \right) \tag{14}$$

since $P_1^*(\varkappa) = 2\varkappa - 1$ and $d\varkappa/dt = 1/t_0$. Using (A3) then gives

$$A_1 = \tfrac{1}{2} \dot{q}_0 t_0 + \sum_{i=2}^{N} g_i A_i, \tag{15}$$

where

$$g_i \triangleq \tfrac{1}{2}(-1)^i \, i(i+1) \equiv \tfrac{1}{2}(-1)^i \, h_i \tag{16}$$

since

$$h_i \triangleq i(i+1). \tag{17}$$

Similarly, the final unknown A_0 can be determined by the formula

$$A_0 = q_0 + \tfrac{1}{2}\dot{q}_0 t_0 + \sum_{i=2}^{N} f_i A_i, \tag{18}$$

where

$$f_i \triangleq \tfrac{1}{2}(-1)^i\,[h_i - 2]. \tag{19}$$

In this way, the initial conditions q_0 and $\dot{q}_0$ are neatly incorporated into the formulation and, in fact, inserting Eqs. (18) and (15) into Eq. (11) then yields

$$q(t) = q_0 + \tfrac{1}{2}\dot{q}_0 t_0 (P_1^* + P_0^*) + \sum_{i=2}^{N} (f_i + g_i P_1^* + P_i^*) A_i \tag{20}$$

as the final form of the assumed solution after the unwanted constants A_0 and A_1 have been eliminated.

Following the same procedure as for the ordinary power series, we assume that the arbitrary function $s(t)$ takes the form

$$s(t) = \sum_{j=2}^{N} (f_j + g_j P_1^*(z) + P_j^*(z))\, a_j. \tag{21}$$

The motivation for this can be viewed in either of two ways:

(i) Since we are solving for only $N-1$ coefficients A_i, for a completely determined system of equations we need only $N-1$ arbitrary constants a_j. (This will be seen more clearly in the sample problems.)

(ii) If we consider $s(t)$ to represent a variation (perturbation) $\delta q(t)$ from the actual path $q(t)$, then, for fixed initial conditions, we obtain

$$\delta A_0 = \sum_{i=2}^{N} f_i\, \delta A_i \triangleq a_0 \tag{22}$$

and

$$\delta A_1 = \sum_{i=2}^{N} g_i\, \delta A_i \triangleq a_1 \tag{23}$$

from Eqs. (18) and (15) respectively. Consequently,

$$s(t) = \sum_{j=0}^{N} a_j P_j^*(z) \tag{24}$$

becomes

$$s(t) = \sum_{j=2}^{N} (f_j + g_j P_1^* + P_j^*)\, a_j, \tag{25}$$

which is identical to the original form (21).

In summary, there are $N+1$ unknowns in Eq. (11) together with two fixed initial conditions given by Eqs. (12). This leaves $N-1$ unknowns A_i as shown in Eq. (20). Thus, for a completely consistent system, only $N-1$ additional constants a_j are needed as given by Eq. (21). Furthermore, it is important to note that the representation given by Eq. (21) is by no means unique. In order to simplify the calculation, $s(t)$ is formulated in terms of Shifted Legendre Polynomials in such a way that $s(0)=s'(0)=0$. Neither of these restrictions is required and, for various problems, other choices might be preferable. In particular, if we retain the P_i^* but drop the simplification of $s(0)=s'(0)=0$, two other admissible series representations are

$$s(t)=\sum_{j=0}^{N-2} a_j P_j^*(z), \tag{21'}$$

$$s(t)=\sum_{j=1}^{N-1} a_j P_j^*(z). \tag{21''}$$

However, a detailed examination of these alternatives is outside the scope of the present paper.

Example I. Damped Harmonic Oscillator

In order to test the application of Eq. (4) in the simplest possible case, the first sample problem considered is the simple damped harmonic oscillator. The appropriate differential equation of motion is

$$m\ddot{x}+c\dot{x}+kx=0, \tag{26}$$

corresponding to a mass m connected to a linear spring with restoring force kx and a linear viscous damper with damping force $c\dot{x}$. For this single degree of freedom test case, the ingredients needed for the function Φ defined in Eq. (1) are

$$\begin{aligned} q_1 &\equiv x, \\ F_1 &= -kx-c\dot{x}, \\ K &= \tfrac{1}{2}m\dot{x}^2, \\ s_1 &\equiv s_x, \end{aligned} \tag{27}$$

so we have

$$\Phi=-(kx+c\dot{x})\,s_x+m\dot{x}\dot{s}_x. \tag{28}$$

Setting $t_1=0$ and $t_2=t_0$ in Eq. (4), we write Hamilton's Law of Varying Action as

$$\int_0^{t_0}\left[-\left(\frac{k}{m}x+\frac{c}{m}\dot{x}\right)s_x+\dot{x}\dot{s}_x\right]dt-\dot{x}s_x\big|_0^{t_0}=0 \tag{29}$$

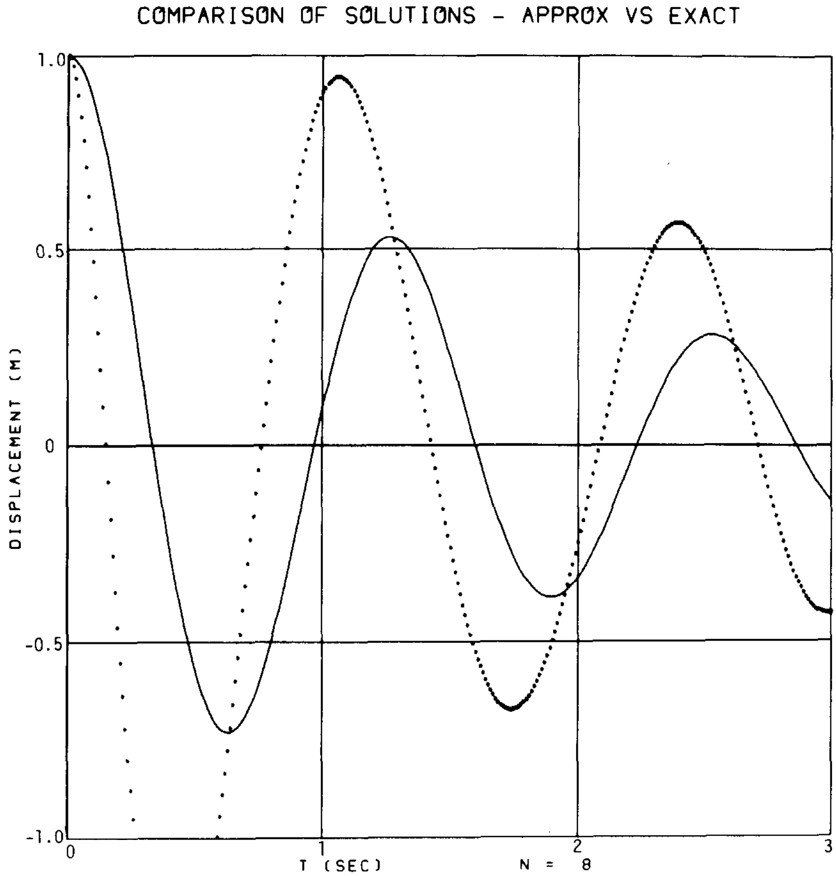

FIG. 1. Exact (solid line) and approximate (dotted line) solutions for the damped harmonic oscillator. The Shifted Legendre Polynomial series contains eight terms ($N = 8$).

after dividing by m. Transforming to the independent variable $\varkappa = t/t_0$ given by Eq. (10), we have

$$\frac{d}{dt}(\varkappa) = (\,\cdot\,) = \frac{d}{d\varkappa}(\;)\frac{d\varkappa}{dt} = \frac{1}{t_0}(\varkappa)' \tag{30}$$

so Eq. (29) becomes

$$-\frac{kt_0^2}{m}\int_0^1 xs_x\,d\varkappa - \frac{ct_0}{m}\int_0^1 x's_x\,d\varkappa + \int_0^1 x's_x'\,d\varkappa = x's_x\,|_0^1. \tag{31}$$

Now, assuming that x and s_x can be represented by the $P_n^*(\varkappa)$ series given in Eqs. (20) and (21), respectively, we find, upon substituting into Eq. (31) and using the orthogonality given by Eq. (A6) in the Appendix together with the two special functions $F_1(n, m)$ and $F_2(n, m)$ defined there by Eqs. (A14) and (A16), that

$$\sum_{j=2}^{N}\left[\sum_{i=2}^{N} M_{ji}A_i - U_j\right] a_j = 0, \tag{32}$$

where

$$M_{ji} \triangleq F_2(j,i) + g_j(2-h_i)\,F_1(i,0) - f_j h_i F_1(i,1) - h_i[1+(-1)^{j+i}]$$
$$-\frac{ct_0}{m}\{2f_j\,g_i + f_jF_1(i,0) + g_jF_1(i,1) + F_1(i,j)\}$$
$$-\frac{kt_0^2}{m}\left\{f_jf_i + \frac{1}{3}\,g_j\,g_i + \frac{\delta_{ji}}{2j+1}\right\}; \tag{33}$$

$$U_j \triangleq \frac{ct_0^2}{m}\dot{x}_0 f_j + \frac{kt_0^2}{m}\{x_0 f_j + \tfrac{1}{2}\dot{x}_0 t_0(f_j + \tfrac{1}{3}g_j)\}; \tag{34}$$

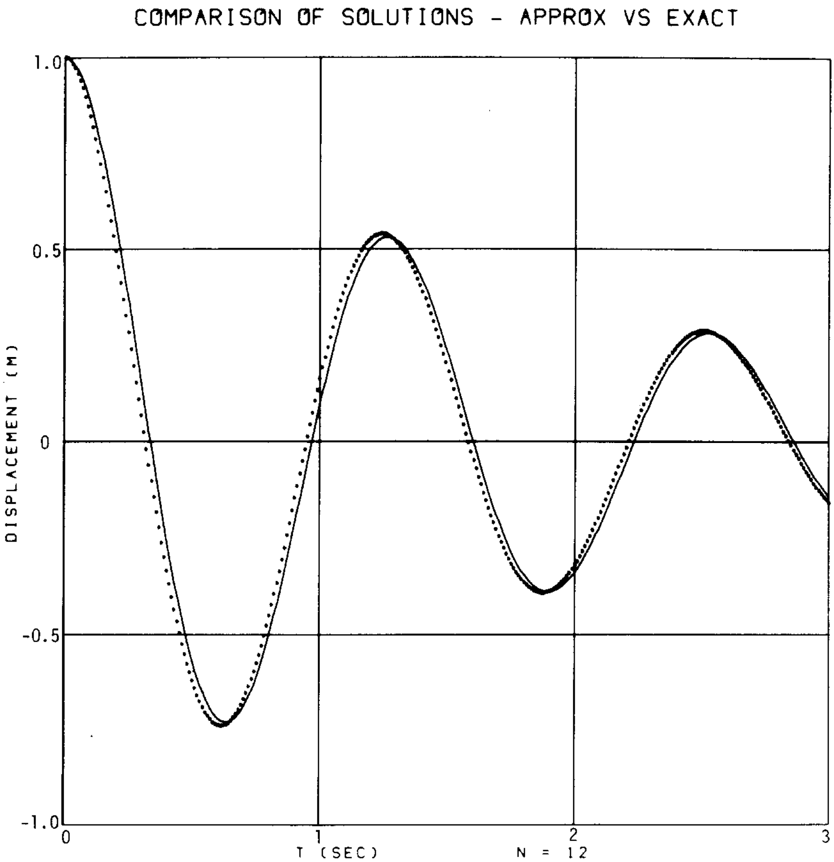

FIG. 2. Exact (solid line) and approximate (dotted line) solutions for the damped harmonic oscillator. The approximating series now has $N = 12$.

and f_j, g_j and h_i have been defined previously in Eqs. (19), (16) and (17). Since Eq. (32) is valid for *any* choice of a_j, it follows that

$$\sum_{i=2}^{N} M_{ji}A_i = U_j \qquad \text{for} \quad j = 2,\ldots, N, \tag{35}$$

which, when written in matrix form, is simply

$$M\mathbf{A} = \mathbf{U}. \tag{36}$$

Next, examining Eq. (33), we see that the matrix elements M_{ji} are completely determined once m, c, k, t_0 and the row and column indices j and i are specified. Similarly, the right-hand-side $\mathbf{U}$ given by (34) is known once m, c, k, t_0, the row

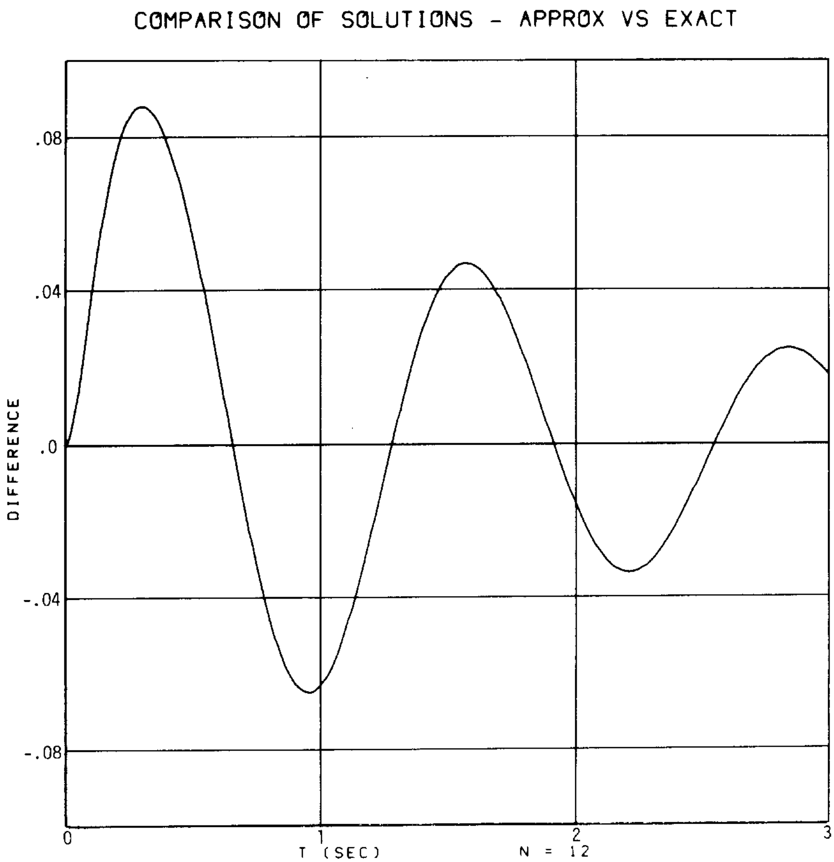

FIG. 3. The difference $\delta(t)$ (defined as the exact solution minus the approximate solution) for the case shown in Fig. 2. For comparison, note that the maximum amplitude in Fig. 2 is 1.0.

index j and the initial conditions x_0 and $\dot{x}_0$ are chosen. Hence, the unknown constants A_i are given explicitly by

$$\mathbf{A} = M^{-1}\mathbf{U}. \tag{37}$$

Numerical tests were performed for the particular case $m = c = 1$ and $k = 25$, corresponding to

$$\ddot{x} + \frac{c}{m}\dot{x} + \frac{k}{m}x = \ddot{x} + 2\zeta\omega_n\dot{x} + \omega_n^2 x = 0 \tag{38}$$

so $\omega_n = 5$ and $\zeta = 0.1$. (The underdamped case was chosen specifically so that "power series" fits would not be easy.) The initial conditions were picked to be $x_0 = 1$, $\dot{x}_0 = 0$ and the final time t_0 was set equal to 3 (so that more than two complete oscillations were included in the solution).

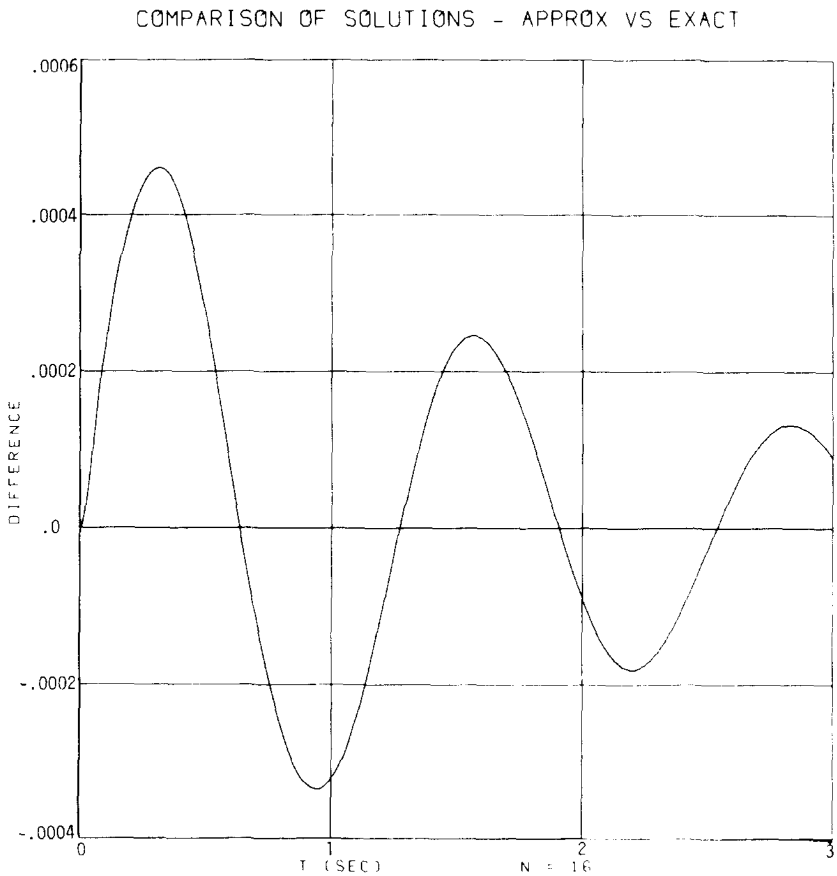

FIG. 4. The difference $\delta(t)$ for the damped harmonic oscillator with $N = 16$ in the approximating series.

Results from the computations are shown in Figs. 1 to 4, where both the approximate and exact solutions are plotted for $N=8$, 12 and 16. For the case $N=16$, the approximate solution is practically identical to the exact solution, so only the difference

$$\delta(t) \triangleq x_E(t) - x_A(t) \tag{39}$$

is shown.

Identical computations were also performed assuming that $x(t)$ could be represented by an ordinary power series

$$x(t) = x_0 + \dot{x}_0 t_0 \varkappa + \sum_{i=2}^{N} A_i \varkappa^i. \tag{40}$$

The analytical development for this situation is given in [2, p.1155] and is not repeated here. Only the results are highlighted in Table I, where we see that the power series is most accurate at $N=12$ and then degrades (always at the end of the interval $0 \leqslant \varkappa \leqslant 1$) as N is increased to 24. This is in *direct contrast* to the $P_n^*(\varkappa)$ series which, as N increases, simply matches the exact solution with greater and greater precision.

The failure of the power series is easily explained, however. The matrix M becomes poorly conditioned as N increases so that, even with computations in double precision (16 decimal digits), the matrix M^{-1} is still determined with unsufficient accuracy for this application.

A second useful comparison is given in Table II where the coefficients for both the power series and the P_n^* series are listed for the case $N=14$. We see that the coefficients steadily decrease in magnitude (in an almost regular fashion) for the P_n^* series while, for the power series, they first increase (by four orders of magnitude!) and then decrease. The former behavior is obviously preferable.

TABLE I

Computational Results for the Simple Harmonic Oscillator[a]

	δ_m	
N	Power series	P_n^* series
8	0.9	1.2
10	0.8	1.1
12	0.08	0.09
14	0.4	0.009
16	0.33	5×10^{-4}
18	3.6(!)	1×10^{-5}
20	26(!!)	2.7×10^{-7}
22	4	4.0×10^{-8}
24	3	2.1×10^{-9}

[a] Maximum fit error $\delta_m = \max_t |x_E - x_A|$ over the time interval $0 \leqslant t \leqslant t_f = 3$.

TABLE II

Coefficient Sets for the Simple Harmonic Oscillator

	Power series	P_n^* series
A_2	$-1.350954323 \times 10^{2}$	$2.358496722 \times 10^{-1}$
A_3	$5.524855061 \times 10^{2}$	$-3.666079243 \times 10^{-1}$
A_4	$-2.042959625 \times 10^{3}$	$5.235500244 \times 10^{-1}$
A_5	$1.983918481 \times 10^{4}$	$-7.227623684 \times 10^{-1}$
A_6	$-8.688759863 \times 10^{4}$	$-4.008240951 \times 10^{-1}$
A_7	$1.385241641 \times 10^{5}$	$7.682819215 \times 10^{-1}$
A_8	$7.962823438 \times 10^{4}$	$2.470680959 \times 10^{-2}$
A_9	$-6.567238125 \times 10^{5}$	$-2.552754118 \times 10^{-1}$
A_{10}	$1.136308555 \times 10^{6}$	$2.615098775 \times 10^{-2}$
A_{11}	$-1.036031059 \times 10^{6}$	$4.332352286 \times 10^{-2}$
A_{12}	$5.430984434 \times 10^{5}$	$-7.591445451 \times 10^{-3}$
A_{13}	$-1.546488164 \times 10^{5}$	$-4.503003244 \times 10^{-3}$
A_{14}	$1.851751331 \times 10^{4}$	$1.322891604 \times 10^{-3}$

Referring now to the error curves shown in Figs. 3 and 4 for the series solution in terms of Shifted Legendre Polynomials, a referee pointed out that these plots look like linearly independent solutions of the equations of motion with the initial conditions $x_0 = 0$, $\dot{x}_0 = v_0 > 0$. Indeed, the two plots are virtually identical except for a change of scale on the ordinate axis. This is caused by the fact that only the single set of polynomials $P_n^*(\varkappa)$ was used to construct the approximating series. As a result, the error is always "orthogonal" to the space spanned by the family of functions and, as N increases, this error is reduced in magnitude but retains its basic form.

EXAMPLE II. RESTRICTED THREE-BODY PROBLEM

Approximate solutions are next constructed for a variety of planar periodic orbits [10] of the restricted three-body problem. Generally, we have limited ourselves to symmetric periodic orbits passing repeatedly near either the smaller, or both, of the two attracting primary masses since orbits of this type have the greatest potential for future space applications [11, 12].

In [5] (in which power series approximations for these orbits were developed), the quantities needed for the function Φ were derived from first principles. Now we will simply list them and refer the reader to [5] for additional detail. Since this problem has two degrees of freedom, we have

$$q_1 = x, \tag{41}$$

$$q_2 = y,$$

$$F_1 = F_x = -(1-\mu)(x+\mu)/r_1^3 - \mu(x+\mu-1)/r_2^3, \tag{42}$$

$$F_2 = F_y = -[(1-\mu)/r_1^3 + \mu/r_2^3]\, y,$$
$$K = \tfrac{1}{2}[\dot{x}^2 + \dot{y}^2 + 2(x\dot{y} - y\dot{x}) + x^2 + y^2], \tag{43}$$

where

r_1 is the distance between the test particle and primary P_1 (of mass $1-\mu$),

$$r_1 = [(x+\mu)^2 + y^2]^{1/2} \tag{44}$$

and

r_2 is the distance between the test particle and primary P_2 (of mass μ),

$$r_2 = [(x+\mu-1)^2 + y^2]^{1/2}. \tag{45}$$

The function Φ is then given by

$$\Phi = \left(\frac{\partial K}{\partial x} + F_x\right) s_x + \left(\frac{\partial K}{\partial y} + F_y\right) s_y + \frac{\partial K}{\partial \dot{x}} \dot{s}_x + \frac{\partial K}{\partial \dot{y}} \dot{s}_y . \tag{46}$$

Letting $t_1 = 0$ and $t_2 = t_0$, Hamilton's Law of Varying Action takes the form

$$\int_0^{t_0} \{[(x+\dot{y}) + F_x]\, s_x + [(y-\dot{x}) + F_y]\, s_y + (\dot{x} - y)\, \dot{s}_x + (x+\dot{y})\, \dot{s}_y\}\, dt$$
$$-(\dot{x} - y)\, s_x \big|_0^{t_0} - (x + \dot{y})\, s_y \big|_0^{t_0} = 0 \tag{47}$$

in this case

Next, assuming that x, y, s_x and s_y can each be represented by series in terms of Shifted Legendre Polynomials, we have

$$x(z) = x_0 + \dot{x}_0 t_0 z + \sum_{i=2}^{N} [f_i + g_i P_1^*(z) + P_i^*(z)]\, A_i,$$
$$s_x = \sum_{j=2}^{N} (f_j + g_j P_1^* + P_j^*)\, a_j, \tag{48}$$
$$y(z) = y_0 + \dot{y}_0 t_0 z + \sum_{k=2}^{M} [f_k + g_k P_1^*(z) + P_k^*(z)]\, B_k,$$
$$s_y = \sum_{l=2}^{M} (f_l + g_l P_1^* + P_l^*)\, b_l,$$

where x_0, y_0, $\dot{x}_0$ and $\dot{y}_0$ denote the initial conditions and A_i $(i = 2,\ldots, N)$, B_k $(k = 2,\ldots, M)$ are dimensionless constants to be determined. Inserting these series and evaluating the resulting integrals in exactly the same way as before for Example I, we obtain the equation

$$\sum_{j=2}^{N}\left[\sum_{i=2}^{N} P_{ji}A_i+\sum_{k=2}^{M} Q_{jk}B_k-U_j\right] a_j + \sum_{l=2}^{M}\left[\sum_{i=2}^{N} R_{li}A_i+\sum_{k=2}^{M} S_{lk}B_k-V_l\right] b_l=0 \tag{49}$$

and, since this is valid for *any* choice of the unknown constants a_j and b_l, we finally get

$$\begin{aligned}\sum_{i=2}^{N} P_{ji}A_i+\sum_{k=2}^{M} Q_{jk}B_k&=U_j \qquad (j=2,\ldots,N),\\ \sum_{i=2}^{N} R_{li}A_i+\sum_{k=2}^{M} S_{lk}B_k&=V_l \qquad (l=2,\ldots,M),\end{aligned} \tag{50}$$

where the matrix elements are

$$\begin{aligned}P_{ji}\triangleq{}& t_0\frac{\delta_{ji}}{2j+1}+\frac{1}{t_0}F_2(j,i)-\frac{1}{t_0}h_i[1+(-1)^{j+i}]\\ &+t_0 f_j f_i+\frac{t_0}{3}g_j g_i+\frac{1}{t_0}g_j[2-h_i]F_1(i,0)\\ &-\frac{1}{t_0}f_j h_i F_1(i,1),\end{aligned} \tag{51}$$

$$\begin{aligned}Q_{jk}\triangleq{}& F_1(k,j)-F_1(j,k)+1-(-1)^{j+k}+2g_jF_1(k,1)\\ &+2f_jF_1(k,0)+4f_j g_k,\end{aligned} \tag{52}$$

$$\begin{aligned}R_{li}\triangleq{}& F_1(l,i)-F_1(i,l)-1+(-1)^{l+i}-2g_lF_1(i,1)\\ &-2f_lF_1(i,0)-4f_l g_i,\end{aligned} \tag{53}$$

$$\begin{aligned}S_{lk}\triangleq{}& t_0\frac{\delta_{lk}}{2l+1}+\frac{1}{t_0}F_2(l,k)-\frac{1}{t_0}h_k[1+(-1)^{l+k}]\\ &+t_0 f_l f_k+\frac{t_0}{3}g_l g_k+\frac{1}{t_0}g_l[2-h_k]F_1(k,0)\\ &-\frac{1}{t_0}f_l h_k F_1(k,1)\end{aligned} \tag{54}$$

and the vector components on the right-hand side are

$$U_j \triangleq -f_j t_0[x_0 + \tfrac{1}{2}\dot{x}_0 t_0 + 2\dot{y}_0] - \tfrac{1}{6} g_j \dot{x}_0 t_0^2$$
$$+ \int_0^{t_0} [(1-\mu)(x+\mu)/r_1^3 + \mu(x+\mu-1)/r_2^3]$$
$$\times [f_j + g_j P_1^*(t/t_0) + P_j^*(t/t_0)]\, dt, \tag{55}$$
$$V_l \triangleq -f_l t_0[y_0 + \tfrac{1}{2}\dot{y}_0 t_0 - 2\dot{x}_0] - \tfrac{1}{6} g_l \dot{y}_0 t_0^2$$
$$+ \int_0^{t_0} [(1-\mu)\, y/r_1^3 + \mu y/r_2^3][f_l + g_l P_1^*(t/t_0) + P_l^*(t/t_0)]\, dt. \tag{56}$$

Examining Eqs. (55) and (56), we now see clearly the essential difficulty caused by the nonlinearities in F_x and F_y for the unknowns A_i and B_k cannot be isolated as in Eq. (37) for the oscillator example. On the other hand, this is easily surmounted by iteration on the computer as described earlier under Approximate Solution.

For these quite sensitive[3] orbit examples, one further refinement was found to be necessary in order to maintain relatively high accuracy over rather long time intervals. We introduce, just as in [5], the idea of "patching" successive series solutions with each series valid over a different portion of the total interval of interest. In other words, for the total time interval

$$0 \leqslant \tau \leqslant \tau_f \tag{57}$$

the solution path is divided into a number of arcs which, with NP equal to the number of "patches," all have the same time duration,

$$t_0 = \tau_{f/NP}, \tag{58}$$

corresponding to the basic interval $0 \leqslant t \leqslant t_0$ for Eq. (4). The new time variable τ is related to t by

$$\tau = (NP - 1)\, t_0 + t \tag{59}$$

so $d/d\tau \equiv d/dt$. After first generating series valid for the interval $0 \leqslant \tau \leqslant t_0$, the patching technique then proceeds by setting $x_0 = x(t_0)$, $\dot{x}_0 = \dot{x}(t_0)$, $y_0 = y(t_0)$ and $\dot{y}_0 = \dot{y}(t_0)$ and repeating the process as before, continuing in this manner until the series corresponding to the interval $(NP-1)\, t_0 \leqslant \tau \leqslant \tau_f$ have been obtained.

In addition, whenever this method is used to produce a series representation of a periodic orbit that is symmetric with respect to the line $y = 0$ (x-axis), it is sufficient to take $\tau_f = \tau^*/2$ (τ^* = orbit period), since the portion of the orbit associated with the

[3] Small perturbations can lead to large deviations in the subsequent motion and, ultimately, destroy the periodicity completely.

interval $\tau^*/2 \leqslant \tau \leqslant \tau^*$ can be constructed from the portion corresponding to $0 \leqslant \tau \leqslant \tau^*/2$ simply by making use of the fact that $x(\tau^* - \tau) = x(\tau)$ and $y(\tau^* - \tau) = -y(\tau)$. Furthermore, such an orbit always makes precisely two perpendicular crossings of the line $y = 0$, one occurring at $t = \tau = 0$ and one at $\tau = \tau^*/2$; hence $y(0) = y(\tau^*/2) = \dot{x}(0) = \dot{x}(\tau^*/2) = 0$.

In order to illustrate this technique, series-generated approximations for two example orbits are included here. First, a retrograde periodic orbit of the Earth–Moon system characterized by the four input values

$$\mu = 0.01215067,$$

$$x_0 = 1.03569,$$

$$\dot{y}_0 = -1.8337259400914745,$$

$$\tau^* = 6.6262745758125766$$

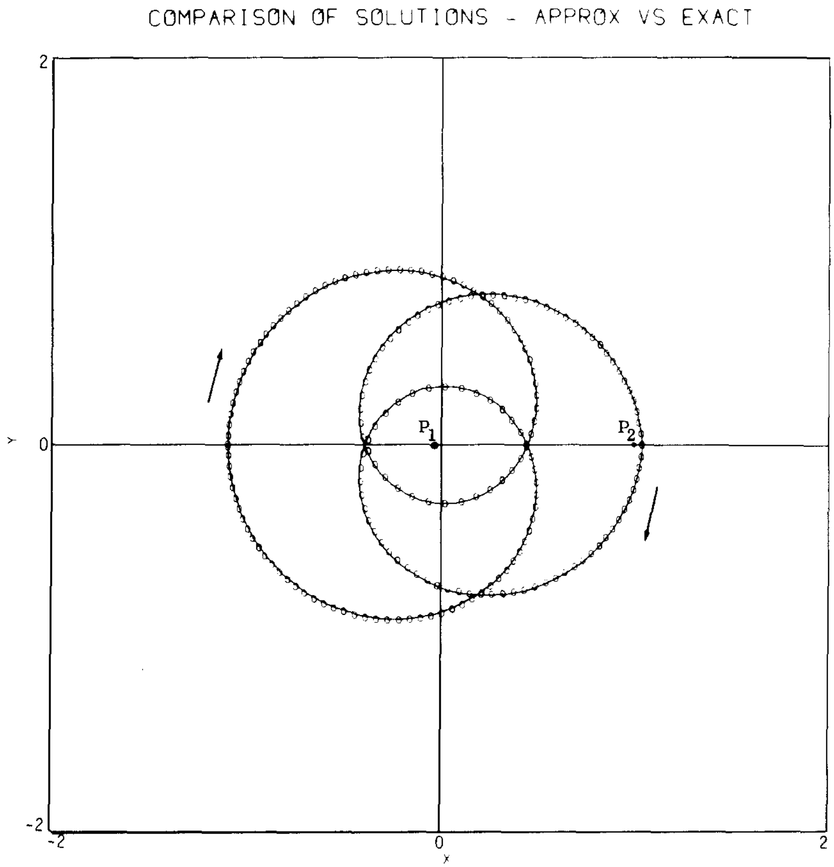

FIG. 5. Exact (solid line) and approximate (solid circles) representations of a retrograde periodic orbit making relatively close passages by both primaries P_1 and P_2.

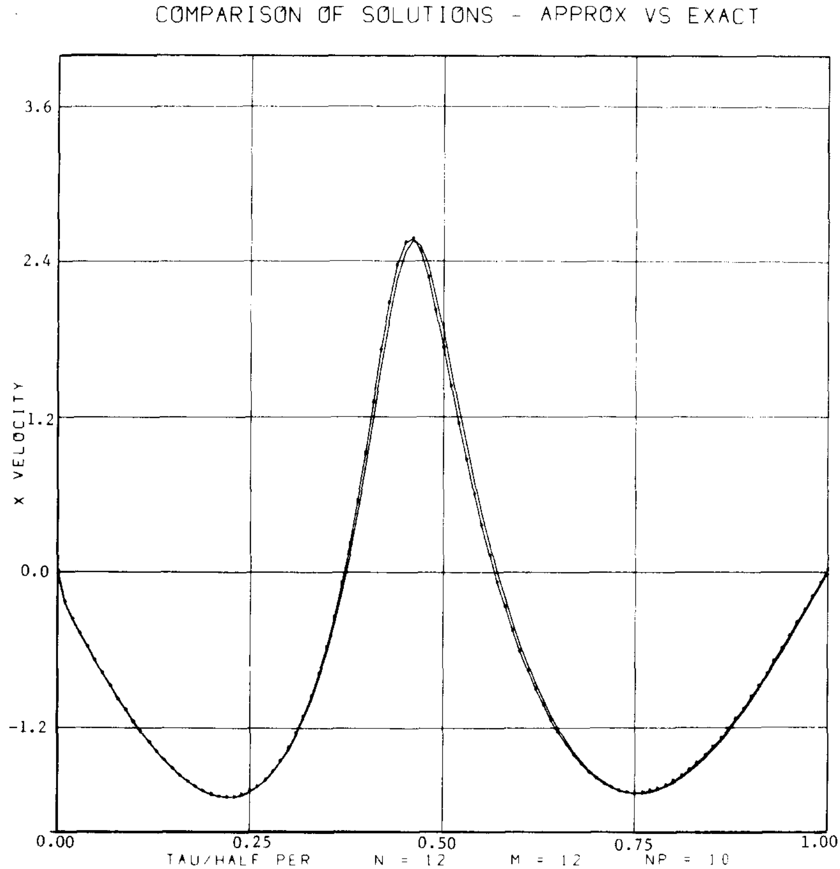

FIG. 6. Exact (solid line) and approximate (dotted line) solutions of $\dot{x}(\tau)$ for the orbit shown in Fig. 5.

is considered. The in-plane stability index κ for this orbit is given by $\kappa = -0.647857$ (an orbit is unstable if the associated value of κ is such that $|\kappa| > 1$). With $N = M = 12$ and $NP = 10$, we obtain the series representation of this orbit shown in Fig. 5 as a sequence of small circles[4]. The exact orbit, produced by numerically integrating the appropriate differential equations of motion, is plotted as a solid line. Clearly, the agreement is remarkably good.

The velocity along the orbit can also be obtained from the approximating series in (48) by differentiating with respect to t. To investigate the agreement for velocity, both the approximate and exact x velocity time histories are plotted in Fig. 6. Again the series representation is found to be quite accurate even though the excursions of $\dot{x}(\tau)$ during half an orbit are rather large.

[4] The portion of this plot associated with the interval $\tau^*/2 \leqslant \tau \leqslant \tau^*$ is formed by simply reflecting the portion corresponding to $0 \leqslant \tau \leqslant \tau^*/2$ about the x-axis.

Next, to examine how the error arising in connection with the P_n^* series representation propagates, Fig. 7 shows the difference $\Delta C \triangleq \bar{C} - C$ between the series-generated Jacobi "constant" $\bar{C}$, given by

$$\bar{C} \triangleq x^2 + y^2 + 2[(1-\mu)/r_1 + \mu/r_2] - \dot{x}^2 - \dot{y}^2, \tag{60}$$

and the actual Jacobi constant for this orbit, $C = 0.1035623354556172$. If the series solution for the orbit were exact, this plot would be a horizontal line, $\Delta C(\tau) = 0$. Instead, we find almost all the error is incurred during the first patch, when the orbit departs from the vicinity of P_2. This then leads to the idea of "adaptive patching" so that the time duration associated with each arc is now no longer constant but depends upon the dynamic behavior and sensitivity of the trajectory during each patch. This, in fact, is a common procedure in accurate numerical integration routines which incorporate variable step sizes.

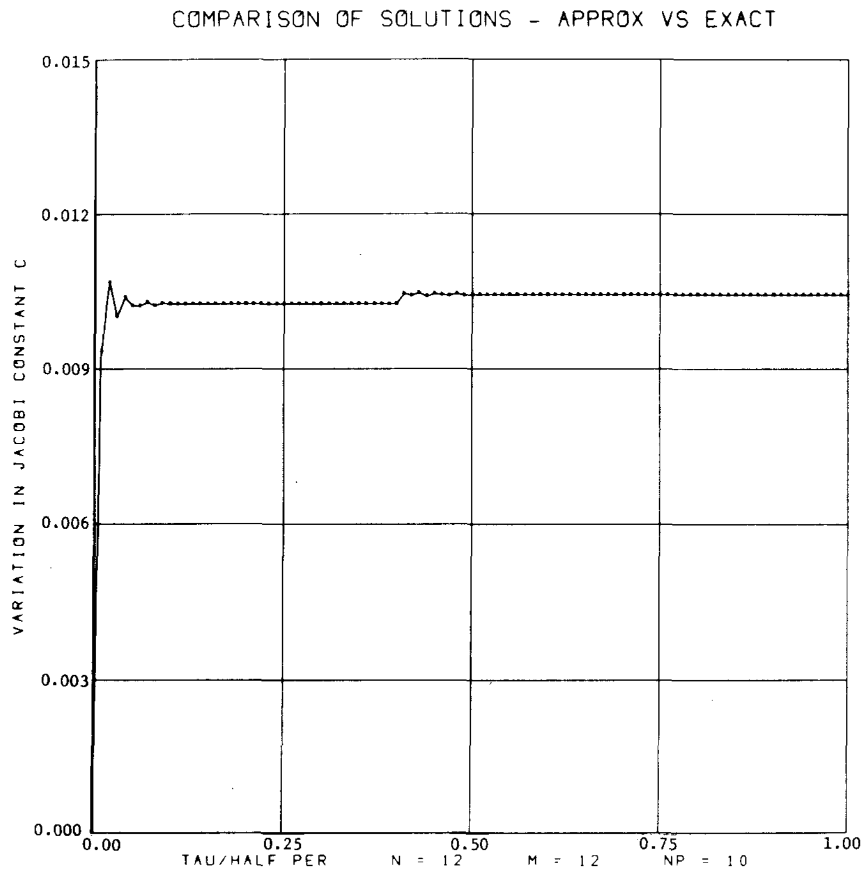

FIG. 7. $\Delta C(\tau)$ for the orbit shown in Fig. 5.

TABLE III

Coefficients of the First Patch for the Retrograde Periodic Orbit Shown in Fig. 5

x Coordinate	y Coordinate
$A_0 = 9.547364764 \times 10^{-1}$	$B_0 = -2.727770587 \times 10^{-1}$
$A_1 = -1.118573513 \times 10^{-1}$	$B_1 = -2.581922326 \times 10^{-1}$
$A_2 = -2.852167991 \times 10^{-2}$	$B_2 = 1.466627634 \times 10^{-2}$
$A_3 = 1.312959370 \times 10^{-3}$	$B_3 = 7.730173504 \times 10^{-4}$
$A_4 = -3.970368837 \times 10^{-4}$	$B_4 = 4.841580894 \times 10^{-4}$
$A_5 = 3.075728948 \times 10^{-4}$	$B_5 = -2.042660976 \times 10^{-4}$
$A_6 = -1.846694645 \times 10^{-4}$	$B_6 = 6.305563350 \times 10^{-5}$
$A_7 = 1.021304408 \times 10^{-4}$	$B_7 = -3.221440650 \times 10^{-6}$
$A_8 = -5.073502226 \times 10^{-5}$	$B_8 = -1.705476150 \times 10^{-5}$
$A_9 = 2.129573684 \times 10^{-5}$	$B_9 = 1.953174222 \times 10^{-5}$
$A_{10} = -6.045594836 \times 10^{-6}$	$B_{10} = -1.544952409 \times 10^{-5}$
$A_{11} = 1.327365736 \times 10^{-7}$	$B_{11} = 8.722395044 \times 10^{-6}$
$A_{12} = 4.250681183 \times 10^{-7}$	$B_{12} = -2.375721296 \times 10^{-6}$

Finally, the numerical values determined for the coefficients A_i and B_k are given in Table III. These apply to the time interval $0 \leqslant \tau \leqslant \frac{1}{10} \tau^*/2$. Note how the coefficients for both the x and y series decrease over several orders of magnitude in an almost monotonic fashion. During each of the 10 patches, a similar behavior was observed. In general, the coefficients dor both the x and y coordinates ranged over 7 to 14 orders of magnitude with the smallest variability occurring during the most sensitive "close approach" segments of the trajectory.

The second example orbit is a direct periodic orbit of the Earth–Moon system making very close passages by both primaries and characterized by

$$\mu = 0.01215067,$$

$$x_0 = 1.0207578217458713,$$

$$\dot{y}_0 = -1.0117456349247884,$$

$$\tau^* = 5.5770155338067978,$$

$$(\kappa = 0.778247).$$

Taking $N = M = 12$ and $NP = 10$, we obtain the plots shown in Fig. 8. Although the two representations of the orbit diverge a little in the left half-plane (i.e., in the vicinity of $\tau^*/2$), the overall agreement is quite good. This is further supported in Fig. 9, where both the approximate and exact y velocity time histories are plotted for half an orbit. The corresponding plot of $\Delta C(\tau)$ is shown in Fig. 10 ($C = 2.6695220566679699$). Two jumps in the error curve are now visible, the first occurring when the orbit departs from the vicinity of P_2 and the second occurring as

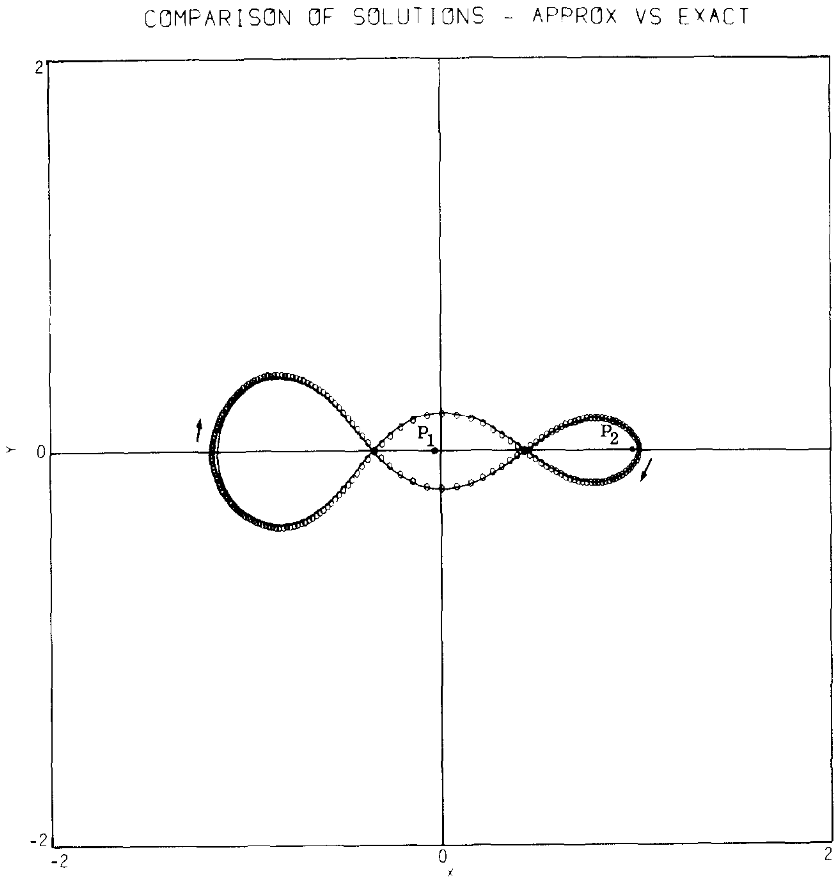

FIG. 8. Exact (solid line) and approximate (solid circles) representations of a direct periodic orbit making very close passages by both primaries P_1 and P_2.

the orbit makes a close passage around P_1. The two plateaux have the values $\Delta C \simeq -0.010$ and $\Delta C \simeq -0.042$, respectively.

For these two orbits, it is of interest to compare the computer time needed to perform an accurate numerical integration of the orbit with that needed to obtain these analytic approximations. Using the UNIVAC 1110 computer at LMSC, a precision numerical integration can be accomplished in less than 10 sec while this implementation of Hamilton's Law required 4 min 27 sec for the retrograde orbit shown in Fig. 5 and 5 min 19 sec for the direct orbit shown in Fig. 8. However, it should be emphasized that this technique is not simply another method of numerical integration but a constructive approach for generating approximate solutions of dynamical problems in analytic form. Hence, its merit for practical applications must rest ultimately on the needs and uses for such series representations. A possible use might be to furnish a highly accurate reference orbit in terms of a set of pre-computed

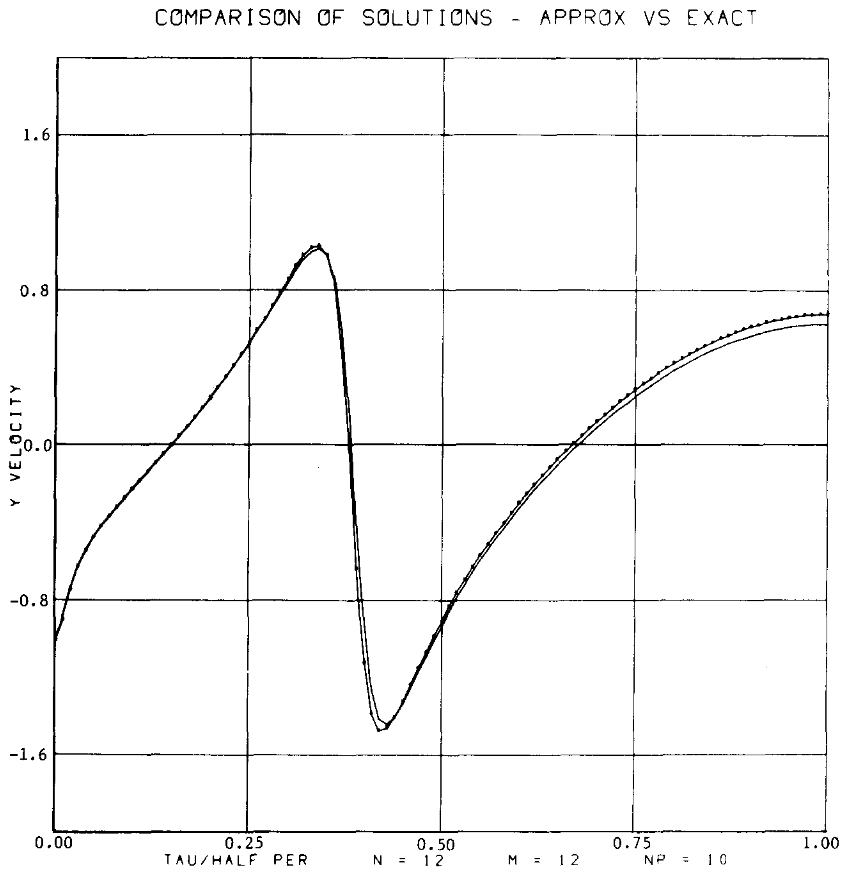

FIG. 9. Exact (solid line) and approximate (dotted line) solutions of $\dot{y}(\tau)$ for the orbit shown in Fig. 8.

coefficients. This would be especially attractive for computations performed on board a satellite which require, for their execution, an accurate (and easily updated!) ephemeris.

CONCLUSIONS AND RECOMMENDATIONS

The method presented in this paper, based on a generalization of Bailey's treatment of Hamilton's Law of Varying Action, shows promise as a technique for obtaining series representations characterizing the motions of dynamical systems. In [5], approximate solutions for three periodic orbits were determined using ordinary power series, as given by Eq. (40), for the x and y coordinates. There, in order to maintain sufficient accuracy, it was found that NP had to be rather large ($\simeq 25$) while N and M

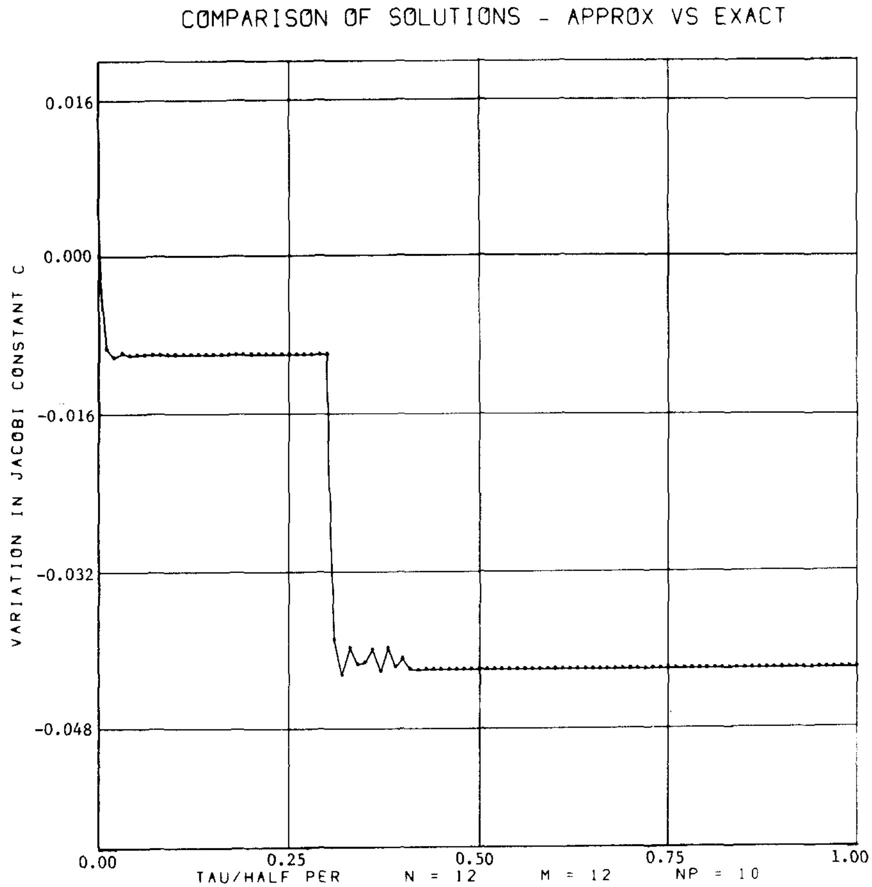

FIG. 10. $\Delta C(\tau)$ for the orbit shown in Fig. 8.

were kept small (=4). Thus, we were forced to use very short arcs with low order series approximations for each arc.

Now, with the use of Shifted Legendre Polynomials as basis functions, the number of arcs has been reduced substantially ($NP = 10$) while the individual series length has been increased to high order ($N = M = 12$). Moreover, the error in the approximate representation (as measured by $\Delta C(\tau)$), has been further decreased. Thus, the use of Shifted Legendre Polynomials has provided a considerable improvement in both the accuracy and efficiency of this method. This is particularly true in the case of the damped harmonic oscillator, where we found, for increasing N, no limit on the accuracy with which the series solution is able to replicate the exact solution.

Based upon the results presented in this paper, a number of topics for further work can be suggested.

1. Because of the close approaches to P_1 or P_2, the use of regularized variables [13] should lead to improvements in accuracy and efficiency.

2. For this application, Shifted Legendre Polynomials seemed to be a natural choice because

(i) The interval of interest, $0 \leqslant t \leqslant t_0$, can always be transformed to $0 \leqslant \varkappa \leqslant 1$.

(ii) The orthogonality led to enormous simplifications in the subsequent analytical developments.

(iii) The uniform weighting $w(\varkappa) \equiv 1$ meant no additional weighting functions would have to be artificially introduced.

(iv) Functions "close" to the analytic solution are not known since, for the orbit examples, no analytic solution is available.

However, other sets of orthogonal functions should be examined. In particular, Shifted Tchebychev Polynomials $T_n^*(\varkappa)$ [8, pp. 774, 778–779] could be advantageous since the nonuniform weighting function

$$w(\varkappa) = (\varkappa - \varkappa^2)^{-1/2} \tag{61}$$

should provide a cure for the higher order discontinuities presently obtained at the patching (or node) points. Also, trigonometric series are another obvious choice for representing these symmetric periodic orbits.

3. At the "patching points," continuity is presently required only for $q(t)$ and $\dot{q}(t)$. In fact, these conditions are sufficient for exact solutions but do not constrain approximate solutions tightly enough. The use of these so-called spline fits should definitely be investigated as, in this context, demanding continuity in some (L, say, with $0 < L \ll N, M$) of the higher derivatives is equivalent to reducing the number of unknown constants A_i, B_k from $N + M - 4$ to $N + M - (4 + 2L)$.

4. By a simple extension of the previous development, three-dimensional orbits can also be treated. This would then give full generality to the algorithm and enable approximate analytic solutions to be generated for a variety of orbits of current interest.

In conclusion, it is hoped that these results will serve to stimulate others to apply Hamilton's Law of Varying Action to their own problems in dynamics.

Appendix: Useful Relationships for Shifted Legendre Polynomials

The ordinary Legendre Polynomials $P_n(x)$ with $n = 0, 1, 2, \ldots$ are valid over the interval $-1 \leqslant x \leqslant +1$. By the transformation

$$\varkappa = \frac{x+1}{2}; \qquad x = 2\varkappa - 1 \tag{A1}$$

the interval is "shifted" to $0 \leqslant x \leqslant 1$ and we speak of the Shifted Legendre Polynomials $P_n^*(x)$. The same boundary conditions apply for both sets, namely,

$$P_n^*(0) = (-1)^n; \qquad P_n^*(1) = 1 \tag{A2}$$

and

$$\frac{dP_n^*}{dx}(0) = (-1)^{n+1}\, n(n+1); \qquad \frac{dP_n^*}{dx}(1) = n(n+1) \triangleq h_n \tag{A3}$$

for the first derivatives.

The first few polynomials are

$$\begin{aligned} P_0^* &= 1, \\ P_1^* &= 2x - 1, \\ P_2^* &= 6x^2 - 6x + 1, \\ P_3^* &= 20x^3 - 30x^2 + 12x - 1, \end{aligned} \tag{A4}$$

and

$$P_4^* = 70x^4 - 140x^3 + 90x^2 - 20x + 1$$

and the following recurrence relation [6, pp. 176–178] or [8, p. 782] is most useful for constructing the necessary polynomials numerically:

$$(n+1)\, P_{n+1}^*(x) = [(4n+2)x - (2n+1)]\, P_n^*(x) - nP_{n-1}^*(x). \tag{A5}$$

Next, because of orthogonality,

$$\int_0^1 P_n^*(x)\, P_m^*(x)\, dx = \frac{\delta_{nm}}{2n+1}, \tag{A6}$$

where δ_{nm} is the usual Kronecker Delta Function.

Now, during the development of approximate solutions to dynamical problems using Hamilton's Law of Varying Action, integrals of the two types

$$\int_0^1 \frac{dP_n^*}{dx} P_m^*\, dx; \int_0^1 \frac{dP_n^*}{dx} \frac{dP_m^*}{dx}\, dx$$

also occur and must be evaluated. Using the known boundary conditions, we have

$$\begin{aligned} \int_0^1 \frac{d}{dx}(P_n^* P_m^*)\, dx &= \int_0^1 \frac{dP_n^*}{dx} P_m^*\, dx + \int_0^1 P_n^* \frac{dP_m^*}{dx}\, dx \\ &= P_n^*(x)\, P_m^*(x)\big|_0^1 \\ &= 1 - (-1)^{n+m}. \end{aligned} \tag{A7}$$

Then, from [6, p. 195], the derivative dP_n^*/dx can be expressed in terms of lower order polynomials by

$$\frac{dP_n^*}{dx} = (4n-2)\,P_{n-1}^* + (4n-10)\,P_{n-3}^* + (4n-18)\,P_{n-5}^* + \cdots, \tag{A8}$$

which, with the definitions

$$[*] \triangleq \text{integer part of } * \tag{A9}$$

and

$$L \triangleq \left[\frac{n+1}{2}\right] \tag{A10}$$

can be written in the convenient form

$$\frac{dP_n^*}{dx} = 2\sum_{l=1}^{L} (2n+3-4l)\,P_{n+1-2l}^*. \tag{A11}$$

The needed integrals can now be evaluated easily. Referring to (A7), we suppose $n > m$ (if not, we simply interchange n and m so this assumption results in no loss of generality). Then (A8) shows that the second integral in (A7) vanishes and, furthermore, that $m \leqslant n-1$ or $n \geqslant m+1$ is required. Hence, making the final definitions

$$p \triangleq n-m-1, \tag{A12}$$

$$S(p) = \begin{cases} 1, & p \geqslant 0, \\ 0, & p < 0, \end{cases} \tag{A13}$$

for a unit step function S, the first required integral

$$\int_0^1 \frac{dP_n^*}{dx} P_m^*\,dx = (1-(-1)^{n+m})\,S(p) \triangleq F_1(n,m) \tag{A14}$$

is obtained in closed form. This formula shows, in fact, that the integral has only the following two integer values

$$\int_0^1 \frac{dP_n^*}{dx} P_m^*\,dx = \begin{cases} 2 & \text{if} \quad m \leqslant n-1 \text{ and } n+m \text{ is odd} \\ 0 & \qquad\qquad \text{otherwise.} \end{cases} \tag{A15}$$

The final integral (of two derivatives) which we need is calculated by inserting (A11) and using the orthogonality given by (A6) to obtain

$$\begin{aligned}\int_0^1 \frac{dP_n^*}{dx}\frac{dP_m^*}{dx}\,dx &= 2\left[\frac{l+1}{2}\right]\left\{2l+1-2\left[\frac{l+1}{2}\right]\right\}\,(1+(-1)^{n+m})\,S(q) \\ &\triangleq F_2(n,m), \end{aligned}\tag{A16}$$

where

$$l \triangleq \min(n, m) \tag{A17}$$

and

$$q \triangleq n + m - 2. \tag{A18}$$

Note that this integral vanishes if $n + m$ is odd and, provided $q \geqslant 0$, attains a simple set of integer values otherwise.

ACKNOWLEDGMENTS

It is a pleasure to acknowledge Dr. D. H. Hodges of the NASA Ames Research Center for initially suggesting the use of Shifted Legendre Polynomials. Also, the author is deeply indebted to Mr. D. A. Levinson for his interest and help with this work. Finally, I am grateful to Mrs. Betty Charles and D. L. Staley for their efforts in typing several versions of this paper.

REFERENCES

1. C. D. BAILEY, A new look at Hamilton's principle, *Foundations Phys.* **5**(1975), 433–451.
2. C. D. BAILEY, Application of Hamilton's law of varying action, *AIAA J.* **13** (1975), 1154–1157.
3. W. R. HAMILTON, On a general method in dynamics, *Phil. Trans. Roy. Soc. London* (1834), 247–308.
4. W. R. HAMILTON, Second essay on a general method in dynamics, *Phil. Trans. Roy. Soc. London* (1835), 95–144.
5. D. L. HITZL AND D. A. LEVINSON, Application of Hamilton's law of varying action to the restricted three-body problem, *Celest. Mech.* in press.
6. G. SANSONE, "Orthogonal Functions," Interscience, New York, 1959.
7. H. HOCHSTADT, "Special Functions of Mathematical Physics," Holt, Rinehart & Winston, New York, 1961.
8. M. ABRAMOWITZ AND I. A. STEGUN (Eds.), "Handbook of Mathematical Functions," Dover, New York, 1965.
9. C. D. BAILEY, Comment on "Unconstrained Variational Statements for Initial and Boundary Value Problems", *AIAA J.* **17** (1979), 541–542.
10. R. A. BROUCKE, Periodic Orbits in the Restricted Three-Body Problem with Earth–Moon Masses," Jet Propulsion Laboratory Technical Report 32–1168, 1968.
11. D. L. HITZL, Generating orbits for stable close encounter periodic solutions of the restricted problem, *AIAA J.* **15** (1977), 1410–1418.
12. D. L. HITZL AND M. HÉNON, The stability of second species periodic orbits in the restricted problem ($\mu = 0$), *Acta Astronautica* **4** (1977), 1019–1039.
13. V. SZEBEHELY, "Theory of Orbits," Academic Press, New York, 1967.